Molecular signatures distinguish human central memory from effector memory CD8 T cell subsets

Molecular Signatures Distinguish Human Central Memory from Effector Memory CD8 T Cell Subsets[1]

Tim Willinger,[2]* Tom Freeman,† Hitoshi Hasegawa,‡ Andrew J. McMichael,* and Margaret F. C. Callan*§

Memory T cells are heterogeneous in terms of their phenotype and functional properties. We investigated the molecular profiles of human CD8 naive central memory (T_{CM}), effector memory (T_{EM}), and effector memory RA (T_{EMRA}) T cells using gene expression microarrays and phospho-protein-specific intracellular flow cytometry. We demonstrate that T_{CM} have a gene expression and cytokine signaling signature that lies between that of naive and T_{EM} or T_{EMRA} cells, whereas T_{EM} and T_{EMRA} are closely related. Our data define the molecular basis for the different functional properties of central and effector memory subsets. We show that T_{EM} and T_{EMRA} cells strongly express genes with known importance in CD8 T cell effector function. In contrast, T_{CM} are characterized by high basal and cytokine-induced STAT5 phosphorylation, reflecting their capacity for self-renewal. Altogether, our results distinguish T_{CM} and T_{EM}/T_{EMRA} at the molecular level and are consistent with the concept that T_{CM} represent memory stem cells. *The Journal of Immunology,* **2005, 175: 5895–5903.**

Immunological memory is a fundamental feature of the adaptive immune system. It enables the immune system to respond more rapidly and vigorously to infectious pathogens that have been encountered previously. In particular, memory CD8 T cells play a major role in host defense by rapid recognition and lysis of virus-infected cells. A memory response differs both quantitatively and qualitatively from a primary response (1–3). Thus, compared with a naive population, the precursor frequency of Ag-specific memory cells is increased and, furthermore, these cells have an enhanced capacity to respond to Ag. Despite recent progress, a clear understanding of the molecular and cellular basis of T cell memory is still lacking.

Within human CD8 T cells, van Lier and colleagues (4) first demonstrated the presence of phenotypically and functionally distinct subsets of primed T cells by analyzing expression of CD27 and CD45RA. Although naive CD8 T cells express both of these cell surface glycoproteins, cells expressing CD27 but not CD45RA were reported to have functional properties suggestive of "memory" cells and those that expressed CD45RA but not CD27 had functional properties suggestive of "effector" cells (4).

Subsequently, Lanzavecchia and coworkers (5, 6) used expression of CCR7 and CD45RA to define subsets of CD8 T cells. According to this scheme, naive T cells (T_N)[3] (3) express both CCR7 and CD45RA whereas primed CD8 T cells can be considered as belonging to one of three different subsets. Two of these lack expression of CD45RA and thus lie broadly within the van Lier memory subset. Of these, central memory cells (T_{CM}) express CCR7 while effector memory (T_{EM}) cells lack expression of CCR7. In humans, but not in mice, there is a third T cell memory subset, T_{EMRA}, that includes cells that express CD45RA but lack expression of CCR7.

T_{CM} and T_{EM} can be distinguished by their different homing and effector capacities (6). Like naive cells, T_{CM} express CD62 ligand (CD62L) and CCR7 and home to secondary lymphoid organs. In contrast, expression of a different set of chemokine receptors (e.g., CXCR3) allows T_{EM} and T_{EMRA} to gain access to inflamed peripheral tissues. Human T_{EM}, and T_{EMRA} in particular, are more differentiated in terms of effector function than T_{CM} (4, 7–11). They display potent ex vivo cytotoxicity and produce Th1 cytokines upon stimulation, whereas T_{CM} mainly produce IL-2 and Th2 cytokines. Further studies have shown that T_{CM} have a higher proliferative potential and greater resistance to apoptosis, whereas T_{EM}/T_{EMRA} have a skewed TCR repertoire and are characterized by a "senescent" replicative history (9, 10, 12–14).

The importance of both T_{CM} and T_{EM} subsets for the control of infectious diseases and the effectiveness of vaccines has been shown in several murine studies (15–17). In mice, Ahmed and colleagues (18) have demonstrated a linear differentiation pathway $T_N \rightarrow$ effector $\rightarrow T_{EM} \rightarrow T_{CM}$ following acute lymphocytic choriomeningitis virus (LCMV) infection. Two other models of CD8 memory T cell differentiation have been proposed: the signal strength/progressive differentiation model by Lanzavecchia and coworkers (6) and the "independent" differentiation model by Pannetier and colleagues (19). However, in humans the developmental relationship among T_{CM}, T_{EM}, and T_{EMRA} is still controversial.

In this study, we have conducted gene expression and kinase phospho-protein profiling of CD8 memory subsets to investigate their molecular programs and their cytokine responsiveness and to

*Medical Research Council Human Immunology Unit, Weatherall Institute of Molecular Medicine, Oxford, United Kingdom; †Medical Research Council Rosalind Franklin Centre for Genomics Research, Wellcome Trust Genome Campus, Hinxton, Cambridge, United Kingdom; ‡University School of Medicine, Shigenobu, Ehime, Japan; and §Division of Medicine, Imperial College London, and Department of Rheumatology, Chelsea and Westminster Hospital, London, United Kingdom

Received for publication June 21, 2005. Accepted for publication August 24, 2005.

The costs of publication of this article were defrayed in part by the payment of page charges. This article must therefore be hereby marked *advertisement* in accordance with 18 U.S.C. Section 1734 solely to indicate this fact.

[1] This work was supported by grants from the Medical Research Council (U.K.) and the Leukaemia Research Fund. T.W. is a Medical Research Council Clinical Research Fellow and M.F.C. is a Medical Research Council Senior Clinical Fellow.

[2] Address correspondence and reprint requests to Dr. Tim Willinger, MRC Human Immunology Unit, Weatherall Institute of Molecular Medicine, The John Radcliffe, Oxford OX3 9DS, U.K. E-mail address: TimW@hammer.imm.ox.ac.uk

[3] Abbreviations used in this paper: T_N, naive T cell; FDR, false discovery rate; GMFI, geometric mean fluorescence intensity; GO, gene ontology; MDS, multidimensional scaling; T_{CM}, central memory T cell; T_{EM}, effector memory T cell; T_{EMRA}, effector memory RA T cell; CD62L, CD62 ligand; LCMV, lymphocytic choriomeningitis virus; ID, identifier.

0022-1767/05/$02.00

gain insight into their relationship at the molecular level. We elected to define memory subsets according to the Lanzavecchia model in view of the capacity of the model to distinguish between two apparently functionally distinct subpopulations of $CD45RA^-$-primed T cells (T_{CM} and T_{EM}) and the extensive debate in the literature concerning the lineage relationship between T_{CM} and T_{EM} or T_{EMRA} cells. Our results define a molecular basis for the different functional properties of human CD8 T cell memory subsets and place T_{CM} cells between T_N and T_{EM}/T_{EMRA} cells in terms of their molecular signatures.

Materials and Methods

Isolation of CD8 T cell subsets

PBMC were obtained from buffy coat preparations from four healthy donors by density gradient centrifugation using LymphoPrep (Nycomed) in accordance with institutional ethics approval. We isolated $CD8^+$ T cells by positive immunomagnetic selection using dynabeads (Dynal) with detachment of the anti-CD8 mAb. Purity of the selected $CD3^+CD8^+$ cells was >98% as assessed by flow cytometry. The $CD8^+$ T cells were then stained with mAbs specific for CCR7 (R&D Systems) and CD45RA (BD Pharmingen) and sorted into T_N ($CCR7^+CD45RA^+$), T_{CM} ($CCR7^+CD45RA^-$), T_{EM} ($CCR7^-CD45RA^-$), and T_{EMRA} ($CCR7^-CD45RA^+$) populations on a MoFlow Cytometer (DakoCytomation). Purity of isolated subpopulations was 93–98%. Cell purification procedures were conducted at 4°C to minimize in vitro-induced changes in gene expression.

Preparation of cRNA and array processing

Total RNA was extracted from purified CD8 T cell populations using TRI reagent (Sigma-Aldrich) followed by RNA cleanup with the RNeasy kit (Qiagen). We confirmed integrity of the total RNA by Lab-on-a-Chip 2100 Bioanalyzer (Agilent) quality control. Double-stranded cDNA was synthesized using a modification of the SMART-PCR protocol described by Petalidis et al. (20). This protocol has been validated regarding the fidelity of amplification and compares favorably with the direct labeling approach in terms of sensitivity, speed and cost-effectiveness. Briefly, 300–600 ng of total RNA was reverse transcribed using a modified SMART CDS Primer IIA containing a 5′ T7 promoter sequence. After double-stranded DNA synthesis, the cDNA was subjected to 15 rounds of PCR according to the manufacturer's recommendations. Biotin-labeled cRNA was generated from 2 μg of double-stranded cDNA by one round of in vitro transcription with the BioArray High Yield RNA Transcript Labeling kit (Enzo). cRNA yields were >50 μg with A_{260}:A_{280} ratios of 1.9–2.1. After fragmentation, labeled RNA was hybridized to Affymetrix HG-U133 plus 2.0 arrays (containing 54,675 probe identifiers (IDs)) according to the manufacturer's instructions. Arrays were scaled to a target intensity of 100 using GCOS software (Affymetrix). Scaling factors for all arrays were within 2 SDs of the mean (range, 0.7–1.2). Percentage of genes as scored present on arrays by GCOS software was 32.8 ± 2.5%. 3′ to 5′ *GAPDH* ratios ranged from 0.8 to 1.2. We performed replicate microarray experiments with RNA from four independent donors. R^2 values derived from scatter plots of signal intensity values were 0.98 or greater for individual replicates of CD8 T cell populations. All data have been deposited in the European Bioinformatics Institute ArrayExpress public database. Accession number: E-TABM-40.

Microarray data analysis

We used the comprehensive software package BRB-ArrayTools (21, 22) for data analysis. First, the robust multiarray average algorithm was applied for probe-level normalization, background correction, and to calculate log expression measures (23). Then, to minimize the negative effects of random noise, we performed the following filtering steps: First, transcripts showing minimal variation across the set of arrays (log intensity variation, $p > 0.01$ with the test hypothesis that gene i has the same variance as the median variance) were removed. Second, transcripts with mostly unreliable expression (GCOS present call ≤4 in 16 samples) were also excluded. This resulted in 10,854 probe IDs that were used for further unsupervised analysis to examine the relationship among samples. First, we used standard average-linkage hierarchical clustering to cluster the samples using the Pearson correlation as the distance metric. Genes were median centered before clustering. The so-called R (reproducibility) measure described in Ref. 24 was used to evaluate the robustness of the clusters. The R measure is based on perturbing the expression data with Gaussian noise, reclustering, and measuring the similarity of the new clusters to the original clusters. R measure = 1 indicates perfect cluster reproducibility. Second, multidimensional scaling (MDS) analysis was conducted using the Pearson correlation to measure between sample distances. MDS is related to principal components analysis and allows the representation of high-dimensional data in three-dimensional space. The Pearson correlation subtracted from unity was used to measure the distance between two CD8 T cell subsets by calculating the average linkage distance (distance range, 0–2) (25). The average linkage distance represents the mean of all pairwise distances (linkages) between samples from the two CD8 subsets concerned.

We identified genes that were differentially expressed among the four CD8 subsets using a random variance F test. The random variance F test permits sharing information among genes about within-class variation without assuming that all genes have the same variance (26). It is therefore well suited to the analysis of microarray data with a relatively small number of replicates. Genes were considered statistically significant if their $p < 0.001$. We used a multivariate permutation test (21) to provide 95% confidence that the false discovery rate (FDR) was <1% (1000 random permutations). The multivariate permutation test is nonparametric and does not require the assumption of Gaussian distributions. Using the significance of microarray analysis algorithm (27) produced similar results. We also performed a global test of whether the expression profiles differed between the different CD8 populations by permuting the labels of which arrays corresponded to which population. For each permutation, the p values were recomputed and the number of genes significant at the 0.001 level was noted. The proportion of the permutations that gave at least as many significant genes as with the actual data was the significance level of the global test.

Gene ontology (GO) overrepresentation analysis

Onto-Express was used to translate gene lists into functional profiles and to identify overrepresented GO annotation categories (28). Multiples (probes corresponding to the same gene) were removed before analysis. Enrichment of GO categories and associated p values were calculated based on hypergeometric distribution statistics. We obtained similar results when applying a χ^2 test. Multiple testing correction was conducted with the Bonferroni step-down (Holm) procedure ($\alpha = 0.05$). The Holm procedure is based on the family-wise error rate and a conservative global measure of type I error.

Analysis of cytokine signaling by phospho-specific intracellular FACS

PBMC were stimulated in serum-free RPMI 1640 (Invitrogen Life Technologies) for 15 min at 37°C in 5% CO_2,with or without cytokines, at the following concentrations: IL-2 (200 U/ml), IL-4, IL-6, IL-7, IL-10, IL-12, IL-15, IL-18, TNF-α, IFN-β, and IFN-γ (all 50 ng/ml). All cytokines were purchased from R&D Systems apart from IL-2 (Biotest), IL-7/TNF-α (PeproTech), and IL-18 (Leinco Technology). We conducted simultaneous staining of PBMC for surface markers and for intracellular phosphorylated STAT and NF-κB proteins according to the protocol developed by Nolan and colleagues (29). Briefly, PBMC were fixed in 1.5% formaldehyde for 10 min at room temperature and permeabilized in methanol for 15 min on ice. This was followed by a rehydration step before staining the cells for 1 h at room temperature. We used CD62L-FITC/-PE, CD45RA-allophycocyanin, and CD8-PerCP Abs for surface staining and phospho-specific Abs STAT1 (Y701)-PE, STAT3 (Y705)-PE, STAT4 (Y693)-Alexa Fluor 488, STAT5 (Y694)-PE, STAT6 (Y641)-Alexa Fluor 488 (all BD Biosciences), NF-κB-p65 (S536)-Alexa Fluor 488 (Cell Signaling Technology) for intracellular staining. Isotype-matched irrelevant Abs were used as controls. Specificity of intracellular phospho-staining was verified by using blocking phospho-peptides (1 μg/sample; Santa Cruz Biotechnology). Geometric mean fluorescence intensities (GMFI) of phospho-STAT/-NF-κB proteins were calculated for both unstimulated and stimulated CD8 T cell subsets. We determined differences in phosphorylation by obtaining the $\log_2$ ratios of GMFI of stimulated vs unstimulated cell populations. Differences in basal phosphorylation were compared by calculating each sample's GMFI $\log_2$ ratio divided by the minimum among all samples. We then performed phosphorylated kinase clustering analysis using Cluster and Treeview programs (Michael Eisen, University of California, Berkeley, CA). One-way ANOVA was used to determine the significance of differences in phosphorylation between CD8 T cell subsets. Post hoc testing was conducted using Tukey's significant difference test ($\alpha = 0.05$).

Results

Relationships between CD8 memory T cell expression signatures

We isolated highly purified $CD8^+$ T_N ($CCR7^+CD45RA^+$), T_{CM} ($CCR7^+CD45RA^-$), T_{EM} ($CCR7^-CD45RA^-$), and T_{EMRA} ($CCR7^-CD45RA^+$) populations from four healthy donors for

gene expression profiling using Affymetrix oligonucleotide microarrays. Unsupervised data analysis methods were used to explore the relationship between CD8 T cell subsets. First, we subjected the 16 samples (four replicates per subset) to hierarchical clustering using a filtered set of 10,854 probe IDs. We found that for both T_N and T_{CM} all four replicates clustered together (Fig. 1*A*). In contrast, T_{EM} and T_{EMRA} samples from the same donors formed individual clusters. Thus, two main clusters could be distinguished: T_N/T_{CM} and T_{EM}/T_{EMRA}. We confirmed the robustness of these two main clusters by obtaining a high overall cluster reproducibility measure (R index = 0.949, dendrogram cut at level of four clusters). Second, we performed MDS analysis to assess the distances between the expression signatures of the CD8 T cell subsets. MDS could separate T_{EM} and T_{EMRA}, but these two populations were still in close proximity (Fig. 1*B*). In contrast, their transcriptional profiles placed T_{CM} replicates between T_N and T_{EM}/T_{EMRA}. We also calculated average linkage distances between T_N and the different memory subsets as a measure for their relatedness. This showed that the gene expression profile of T_{CM} was closer to T_N than were the profiles of T_{EM} or T_{EMRA} (Fig. 1*C*). Furthermore, we determined the number of differentially expressed genes between the CD8 T cell subsets by individual pairwise comparisons: It was highest for T_N vs T_{EMRA} and T_{CM} vs T_{EMRA} and lowest for T_{EM} vs T_{EMRA} (data not shown), again confirming the dichotomy T_N/T_{CM} vs T_{EM}/T_{EMRA}. Finally, we conducted a global permutation test to assess whether gene expression profiles between the CD8 subsets differed. The significance values (T_{EM} vs T_{EMRA} $p = 0.05714$; all other pairwise comparisons $p = 0.02857$) again suggest that T_{EM} and T_{EMRA} have the most similar gene expression profiles among all CD8 T cell subsets. In summary, analysis of our results, using several different approaches, indicate that the T_{EM} and T_{EMRA} subsets are closely related, whereas T_{CM} have an expression signature that is distinct from that of the other primed T cells and is more closely related to the T_N population.

Genes differentially expressed between CD8 T cell memory subsets

Next, we identified genes that showed significant differential expression among the four CD8 T cell subsets. We used stringent statistical criteria, including a permutation test to minimize the FDR (see *Materials and Methods*). A total of 2092 probe IDs corresponding to 940 named genes met our criteria for differential expression: $p < 0.001$, FDR <1% with 95% confidence.[4] Hierarchical clustering of the differentially expressed genes revealed six main clusters (Fig. 2). Number of probe IDs in each cluster was as follows: 103 (cluster 1), 1369 (cluster 2), 92 (cluster 3), 16 (cluster 4), 129 (cluster 5), and 383 (cluster 6). Two major patterns could be identified among the clusters: First, genes with low expression in T_N with increasing expression from $T_{CM} \rightarrow T_{EM} \rightarrow T_{EMRA}$ (clusters 2 and 3), termed "effector memory signature."[4] Second, genes with high expression in naive cells with decreasing expression from $T_{CM} \rightarrow T_{EM} \rightarrow T_{EMRA}$ (clusters 5 and 6), termed "naive signature."[4] Cluster 1 consisted of genes with higher expression in T_{CM} and T_{EM}.[4] Cluster 4 comprised genes with a "T_{CM}-specific" expression pattern. Surprisingly, very few genes fell within this category and probe IDs for *CD28* accounted for 3 of the 16 included in this cluster (Fig. 2). Overall, >70% of all differentially expressed genes had expression levels in T_{CM} that were intermediate between their expression levels in the T_N population and the T_{EM} and T_{EMRA} subsets. These analyses again suggest that, at the

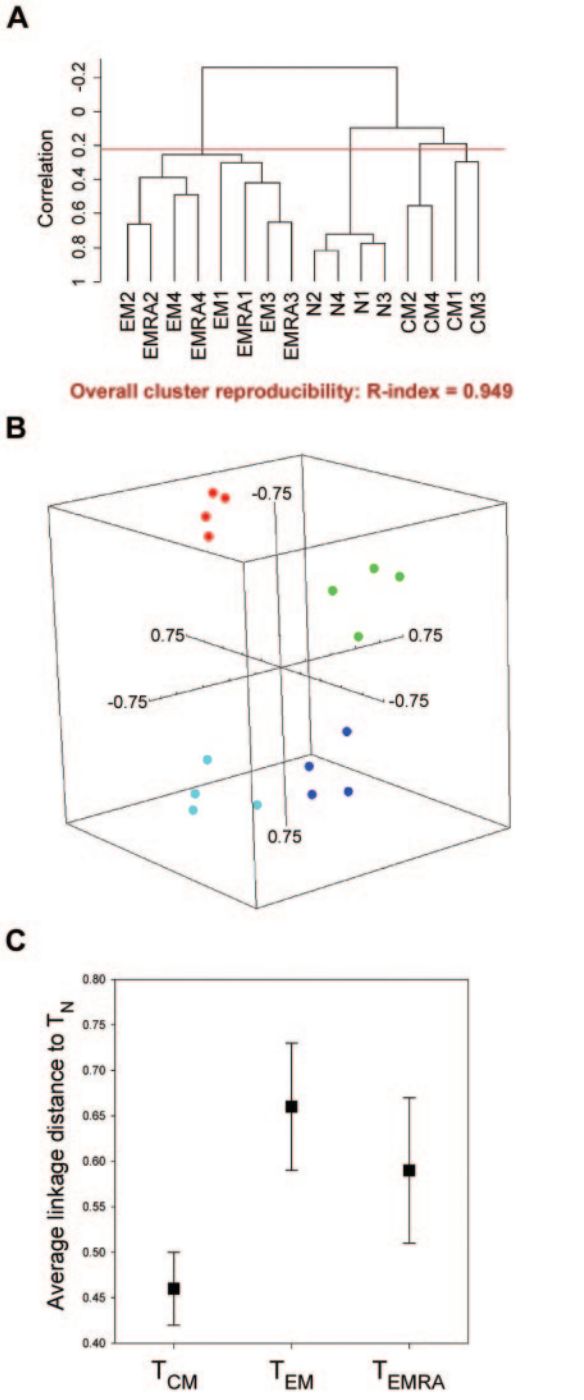

FIGURE 1. Relationships between CD8 memory T cell expression signatures. *A*, Hierarchical clustering of CD8 T cell subset replicates. Average linkage clustering using the Pearson correlation distance was performed based on a set of 10,854 probe IDs (filtered for random noise) from Affymetrix HG-U133 Plus 2.0 gene chip experiments. Overall cluster reproducibility was assessed using the R index (*see Materials and Methods*). The red line indicates the level at which the dendrogram was cut to calculate the R index. *B*, MDS analysis of CD8 T cell subset replicates. The three-dimensional plot shows between-sample distances calculated with the Pearson correlation metric using the same gene set as in *A*. Each dot represents a single replicate sample. Color coding: T_N (red), T_{CM} (green), T_{EM} (dark blue), and T_{EMRA} (light blue). *C*, Average linkage distances between CD8 T_N and memory subsets. Average linkage distances between each CD8 memory T cell subset and T_N were calculated as described in *Materials and Methods* based on the same gene set as in *A* and *B*. Error bars represent SEs (SD of pairwise linkages divided by the square root of the number of linkages).

[4] The online version of this article contains supplemental material.

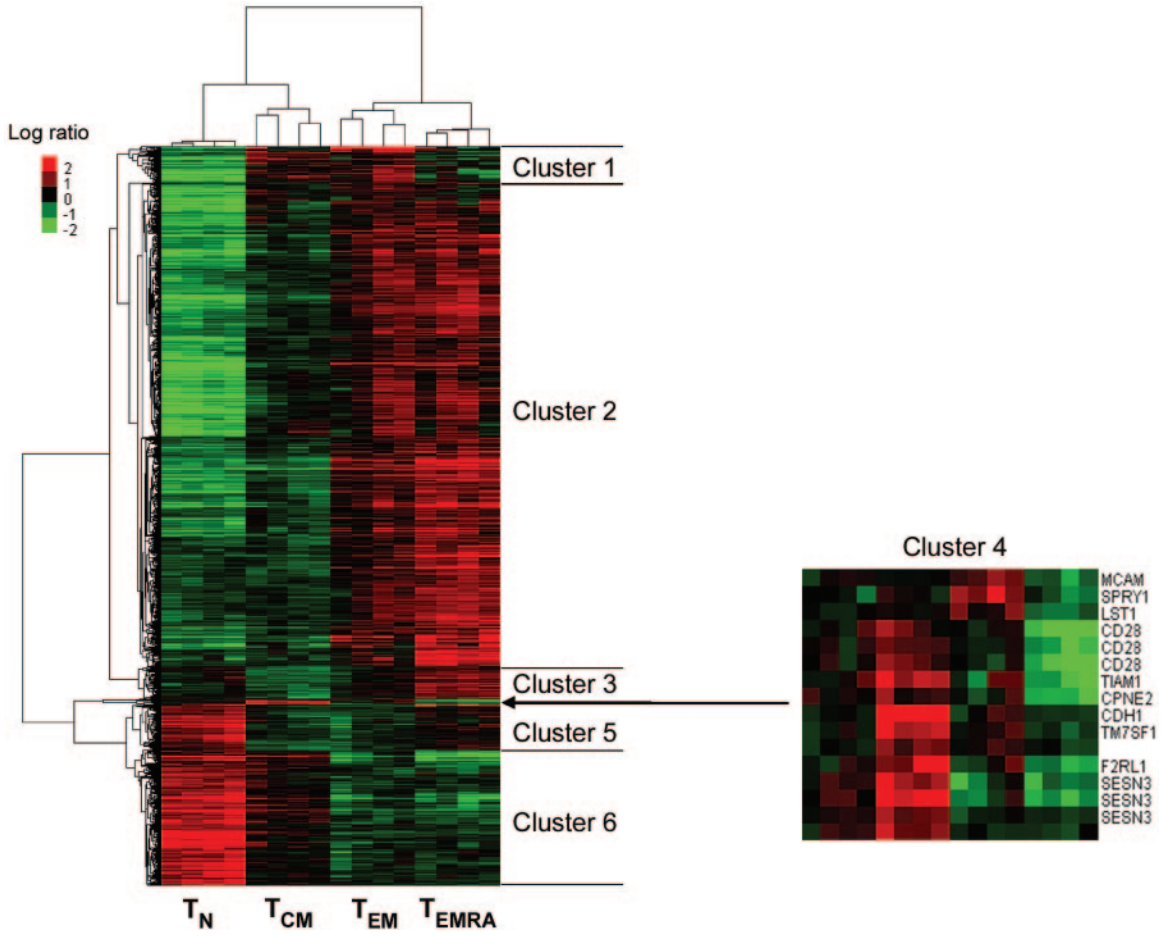

FIGURE 2. Two-way hierarchical clustering of CD8 subset samples and differentially expressed genes. A set of 2092 probe IDs (corresponding to 940 genes) was identified as differentially expressed between CD8 T cell subsets ($p < 0.001$, FDR <1% with 95% confidence) and used for clustering. Each row in the heat map represents a gene and each column a CD8 subset sample. As shown in the color bar, red indicates higher than median expression (up-regulation) and green indicates lower than median expression (down-regulation). The six main gene clusters are indicated on the *right*. Higher magnification of cluster 4 is displayed on the *right*. Gene symbols are shown next to the heat map.

level of gene expression, T_{CM} represent a differentiation state that is intermediate between T_N cells and the T_{EM} and T_{EMRA} subsets.

The effector memory signature of human CD8 T cells

Genes in clusters 2 and 3 (effector memory signature) appear to represent genes that underpin the known high effector capacity of T_{EM} and T_{EMRA}. We identified GO categories that displayed statistical overrepresentation among cluster 2 and 3 genes (hypergeometric statistics, Holm multiple testing correction, $\alpha = 0.05$): GO Biological Processes such as "immune response," "cellular defense response," "cytolysis," and "protein transport" were overrepresented among the effector memory signature genes (Table I). Thus, T_{EM} and T_{EMRA} highly expressed genes encoding lytic granule proteins like *granzyme A* (*GZMA*), *granzyme B* (*GZMB*), *granzyme H* (*GZMH*), and *perforin* (*PRF1*) as well as *TNFSF10* (*TRAIL*) and *TNFSF6* (*FASL*) that mediate perforin-independent apoptosis of target cells.[4] Also T_{EM} and T_{EMRA} showed strong expression of genes involved in protein sorting to granules and granule transport/exocytosis such as *HPS3*, *MYO5A*, *RAB27A*, and *RABGGTA*. Humans with genetic defects of any of these genes have impaired T cell cytotoxicity (30). Finally, genes encoding inflammatory cytokines (e.g., *IFNG* (*IFNγ*)) and chemokines (e.g., *CCL5* (*RANTES*)) were also present in clusters 2 and 3. Consistent with this, in T_{EM} and T_{EMRA} subsets, we found higher expression of transcription factors that control effector function in CD8 T cells (31), i.e., *EOMES*, *TBX21* (*T-BET*), *REL*, *NFATC2*, and *NFATC3*.[4]

In the case of some proteins, particularly those expressed at the cell surface, Abs capable of detecting expression are available. Using these we have confirmed higher expression of CCR7, CD62L, CD27, and CD28 in T_N and T_{CM} subsets at the protein level (data not shown). Apart from effector molecules, differential expression of other genes from clusters 2 and 3[4] between different CD8 T cell subsets has previously been described at the protein level: *ITGAL* (*CD11a*), *ITGB2* (*CD18*), *ITGAM* (*CD11b*), *ITGA4* (*CD49d*), *KLRB1* (*CD161*), *KLRD1* (*CD94*), killer Ig-like receptor family members, and *TNFRSF6* (*CD95*). Therefore, the results of the protein expression studies are consistent with the results of our gene expression study. Overall, this further strengthens the validity of our gene expression data.

Cytokine signaling signatures of CD8 T cell memory subsets

We observed differential expression of cytokine receptor mRNA in our microarray analysis (Table II). For example, naive CD8 T cells were characterized by higher expression of receptors for IL-6 (*IL-6ST*) and IL-7 (*IL-7R*). In contrast, T_{EM} and T_{EMRA} showed preferential expression of receptors for IL-2 family cytokines (*IL-2RB*,

Table I. *GO categories overrepresented in effector memory signature (clusters 2 and 3)*[a]

GO Biological Process	No. of Genes	*p*
Immune response	47	0
Cellular defense response	15	0.000000002
Intracellular signaling cascade	35	0.000000304
Signal transduction	66	0.000000563
Cell growth and/or maintenance	29	0.000028800
Cell motility	13	0.000432000
Response to stress	10	0.001663760
Cytolysis	3	0.002187597
Nucleobase, nucleoside, nucleotide, and nucleic acid metabolism	6	0.010724858
Cell surface recepton-linked signal transduction	12	0.011990255
Protein transport	15	0.012280396
Cell matrix adhesion	8	0.015343897
Lipid transport	6	0.015350114
Response to oxidative stress	5	0.020518426
Cell proliferation	16	0.034058535
DNA metabolism	3	0.040130732

[a] The association of genes from clusters 2 and 3 (Fig. 2) with biological processes was analysed using Onto-Express. Biological processes (GO tree levels 4 and 5) with a total number of three or more genes and $p < 0.05$ are displayed.

IL-2RG) and for inflammatory Th1-type cytokines (*TNFR2*, *IL-12RB1*, *IL-18R1*, *IL-18RAP*, *IFNGR1*). This prompted us to investigate cytokine signaling in CD8 T cell subsets at the single-cell level using multiparameter flow cytometry (32, 33). In doing so, we aimed to generate a functional data set that could be subject to clustering and scaling analysis and give further insight into the relationship between the T_{CM} and T_{EM}/T_{EMRA} subsets.

Activated STAT and NF-κB proteins that transduce cytokine signals were detected with phospho-specific Abs by intracellular FACS staining. Methanol permeabilization can compromise detection of some surface Ags (29), and we observed loss of discrimination for CCR7 surface staining (data not shown). Therefore, we substituted CCR7 with CD62L as a surface marker to identify CD8 T cell subsets in conjunction with CD45RA. CCR7 and CD62L expression largely overlap in CD8 T cells (Ref. 10, and own data not shown). In all, for each of the four T cell subsets, we analyzed basal expression levels of intracellular phosphorylated STAT1, STAT3, STAT4, STAT5, STAT6, and NF-κB. We also analyzed expression levels of phosphorylated STAT1 in cells stimulated with IFN-β or IFN-γ, phosphorylated STAT3 in cells stimulated with IL-6 or IL-10, phosphorylated STAT4 in cells stimulated with IL-12 or IFN-β, phosphorylated STAT5 in cells stimulated with IL-2, IL-7, or IL-15, phosphorylated STAT6 in cells stimulated with IL-4, and phosphorylated NF-κB in cells stimulated with IL-18 or TNF-α. Examples of phospho-specific intracellular staining are shown in Fig. 3. Interestingly, ex vivo CD8 T cells had elevated levels of P-STAT1 and P-STAT5, which could be increased further by cytokine stimulation (Fig. 3*A*). We confirmed specificity of intracellular phospho-staining by using blocking phospho-peptides (data shown). In addition, we found

Table II. *Expression of cytokine receptor mRNA in CD8 T cell subsets*[a]

Gene Symbol	*p*	T_N	T_{CM}	T_{EM}	T_{EMRA}
IL6ST	<0.000000	596.9	235.2	164.9	171.3
		1.0	**0.4**	**0.3**	**0.3**
TGFBR1	<0.000000	349	197.5	465.1	853.6
		1.0	**0.6**	**1.3**	**2.4**
TGFBR3	0.0000003	302.1	1065.7	1541.1	2021.2
		1.0	**3.5**	**5.1**	**6.7**
IL10RA	0.0000016	571.6	1034.8	1393.5	1299.4
		1.0	**1.8**	**2.4**	**2.3**
TGFBR2	0.0000022	233.6	141.5	123.5	126.8
		1.0	**0.6**	**0.5**	**0.5**
IL2RB	0.0000024	933.5	2021.4	2767.1	2859
		1.0	**2.2**	**3.0**	**3.1**
TNFRSF1B	0.0000034	181.6	480.3	763.9	775.6
		1.0	**2.6**	**4.2**	**4.3**
IL18RAP	0.0000074	136.3	366.3	966.5	902.4
		1.0	**2.7**	**7.1**	**6.6**
ACVR1C	0.0000168	201.5	124.9	97.1	84.5
		1.0	**0.6**	**0.5**	**0.4**
CRLF3	0.0000191	1655.5	851	1077.4	1299.3
		1.0	**0.5**	**0.7**	**0.8**
IL18R1	0.0000288	39.1	73.9	108.4	110.7
		1.0	**1.9**	**2.8**	**2.8**
IL12RB1	0.0001641	496.3	577.6	900.6	982.4
		1.0	**1.2**	**1.8**	**2.0**
IL27RA	0.0001734	220.8	115	151.3	215.5
		1.0	**0.5**	**0.7**	**1.0**
IL2RG	0.0002810	1743.4	1458.7	1978.9	2416
		1.0	**0.8**	**1.1**	**1.4**
IFNGR1	0.0003961	689.7	1031.9	1461.6	1241.3
		1.0	**1.5**	**2.1**	**1.8**
ACVR2	0.0004012	431	646.3	345.8	343.8
		1.0	**1.5**	**0.8**	**0.8**
IL7R	NS	3699.1	2732.9	2189.8	1348.6
		1.0	**0.7**	**0.6**	**0.4**
IL4R	NS	734.8	858.5	709.9	539.7
		1.0	**1.2**	**1.0**	**0.7**

[a] This table lists differentially expressed genes encoding cytokine receptors. Gene expression values (RMA expression measures), fold change values relative to T_N (in bold), and associated *p* are shown.

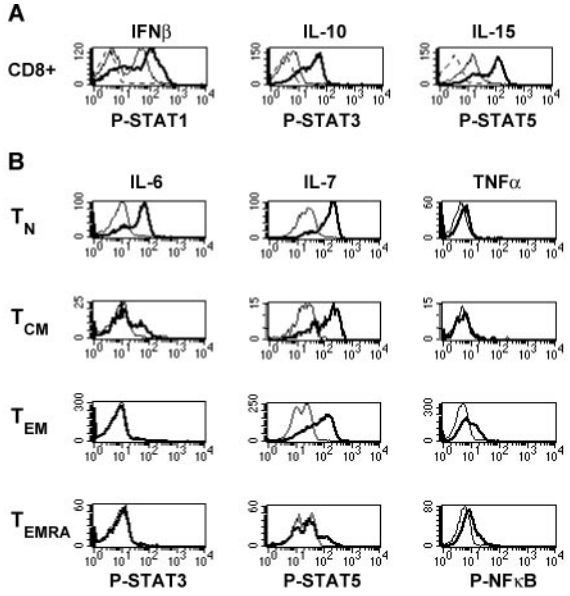

FIGURE 3. Analysis of cytokine signaling in CD8 T cell subsets by phospho-specific intracellular FACS. *A*, Phospho-STAT proteins were detected in unstimulated or cytokine-stimulated PBMC after staining with Abs for CD8 and P-STAT. A representative example from one donor is shown for STAT1, STAT3, and STAT5 phosphorylation in response to IFN-β, IL-10, and IL-15, respectively (thick line histograms). Thin line histograms indicate basal phosphorylation and dashed line histograms indicate isotype control staining. Histograms are gated on $CD8^+$ lymphocytes. *B*, Phospho-STAT/NF-κB proteins were detected in unstimulated or cytokine-stimulated PBMC after staining with Abs for CD8, CD62L, CD45RA, and P-STAT/P-NF-κB. Gating of $CD8^+$ cells based on CD62L/CD45RA expression was used to define T_N, T_{CM}, T_{EM}, and T_{EMRA} subsets. A representative example from one donor is shown for STAT3, STAT5, and NF-κB phosphorylation in response to IL-6, IL-7, and TNF-α, respectively (thick line histograms). Thin line histograms indicate basal phosphorylation.

that, as known from the literature, some cytokines did not induce phosphorylation of certain STAT proteins, e.g., STAT1 and STAT3 in response to IL-4 or STAT5 and STAT6 in response to IL-10 (data not shown). Importantly, in T_N and T_{CM}, we observed high STAT3 phosphorylation in response to IL-6 and in T_N, T_{CM}, and T_{EM}, we observed high STAT5 phosphorylation in response to IL-7 (Fig. 3*B*). In contrast, TNF-α induced higher NF-κB phosphorylation in T_{EM}/T_{EMRA}. These results are in line with the differential mRNA expression of receptors for IL-6, IL-7, and TNF-α derived from the microarray data.

In all we performed experiments on samples of blood taken from 10 different donors and found differences in levels of basal STAT/NF-κB phosphorylation between the four different T cells subsets. Interestingly, T_{CM} were characterized by significantly higher cumulative basal STAT/NF-κB phosphorylation compared with T_{EM} and T_{EMRA} subsets (T_{CM} vs T_{EM}, $p = 0.006$, T_{CM} vs T_{EMRA}, $p = 0.001$, one-way ANOVA/Tukey's post hoc test). We also found higher basal P-STAT1 ($p = 0.037$) and P-STAT5 levels ($p = 0.013$) in T_{CM} compared with T_{EMRA}.

Furthermore, the four different T cell subsets responded differently, in terms of changes in STAT/NF-κB phosphorylation, to stimulation with cytokines (Fig. 4). Despite their already elevated P-STAT5 levels, overall T_{CM} had higher induction of STAT5 phosphorylation in response to IL-2 family cytokines (IL-2: T_{CM} vs T_N, $p < 0.001$, T_{CM} vs T_{EM}, $p = 0.044$, T_{CM} vs T_{EMRA}, $p < 0.001$; IL-7: T_{CM} vs T_{EMRA}, $p < 0.001$, IL-15: T_{CM} vs T_N, $p = 0.002$, T_{CM} vs T_{EMRA}, $p = 0.011$). In T_N we detected strong phosphorylation of STAT1 in response to IFN, STAT3 in response to IL-6, STAT5 in response to IL-7, and STAT6 in response to IL-4. Overall, T_N and T_{CM} displayed the highest cumulative cytokine-stimulated phospho-response (T_N vs T_{EMRA}, $p = 0.01$, T_{CM} vs T_{EMRA}, $p = 0.02$). Finally, we found preferential phosphorylation of NF-κB in response to IL-18 and TNF-α in the T_{EM} and T_{EMRA} subsets (IL-18: T_{EM} vs T_N, $p < 0.001$, T_{EM} vs T_{CM}, $p < 0.001$, T_{EM} vs T_{EMRA}, $p = 0.008$; TNF-α: T_{EM} vs T_N, T_{EM} vs T_{CM}, T_{EMRA} vs T_N, and T_{EMRA} vs T_{CM}, all $p < 0.001$). Thus, human CD8 T cell subsets are characterized by the differential activation of cytokine signaling pathways.

We clustered CD8 T cell subsets based on their cytokine signaling profiles. The 18-parameter phospho-signature, based on the 6 basal and 12 stimulated levels of phosphorylated STAT and NF-κB molecules, again placed T_{CM} between T_N and the T_{EM} and T_{EMRA} subsets (Fig. 5*A*). Interestingly, the responses to the proinflammatory cytokines IL-12, IL-18, and TNF-α clustered together and formed a bigger cluster with IL-10 and IL-15. In contrast, IFNs were found in a cluster with IL-4, IL-6, and IL-7. We also performed MDS analysis based on our FACS phospho-proteome data. Similar to the gene expression data, T_{CM} took up an intermediate place between T_N and T_{EM}/T_{EMRA} (Fig. 5*B*). Consistent with this, the average linkage distance between T_{CM} and T_N was smaller than that between T_{EM} or T_{EMRA} and T_N (Fig. 5*C*). Thus, the cytokine signaling signatures support the observations from transcriptional profiling in terms of the molecular relationship of CD8 memory cells.

Discussion

In this study, we identified both the gene expression and cytokine signaling profiles of CD8 T_N, T_{CM}, T_{EM}, and T_{EMRA} cells. Our results provide a molecular basis for the different functional properties of different memory subsets, especially in terms of their self-renewal and effector capacity. They also shed light on the relationship between the primed T cell subsets.

In contrast with a recent study (34) that used the van Lier classification of CD8 T cells, we used the Lanzavecchia model as a basis for our experiments. This allowed us to compare the properties of the T_{CM} subset with those of other T cell populations. Interestingly, we found a clear dichotomy between T_{CM} and the two effector memory (T_{EM} and T_{EMRA}) CD8 T cell subsets at the molecular level. Analysis of both gene expression and cytokine signaling showed that T_{CM} cells were significantly more closely related to T_N cells than T_{EM} or T_{EMRA} cells were. Furthermore, the results of the gene expression analysis imply that T_{CM} cells form a population that is broadly intermediate between T_N and T_{EM} or T_{EMRA} cells. The observation that there are very few truly "T_{CM}-specific" genes is most consistent with the idea that these cells form part of a continuum of differentiation or functional states (35–37). However, it is possible that some of the defining features of T_{CM} are epigenetically imprinted, but not yet actively transcribed, and are therefore not identified by transcriptional profiling.

In many respects, the genetic profile of CD8 T_{CM} cells suggests they are equipped with features of both naive and effector memory cells. Thus, T_{CM} possess some stem cell-like qualities, such as a high proliferative capacity, that are also found in the T_N cell population. In this regard, T_{CM} displayed high basal and IL-2 family-induced STAT5 phosphorylation. Cytokines of the IL-2 family, which mainly signal through STAT5, are known to play an important role in the differentiation and homeostasis of CD8 T cells (38, 39). Thus, IL-15 can induce the homeostatic proliferation of CD8 memory T cells, whereas IL-7 has recently been implicated in the survival of murine CD8 memory precursors, which can be

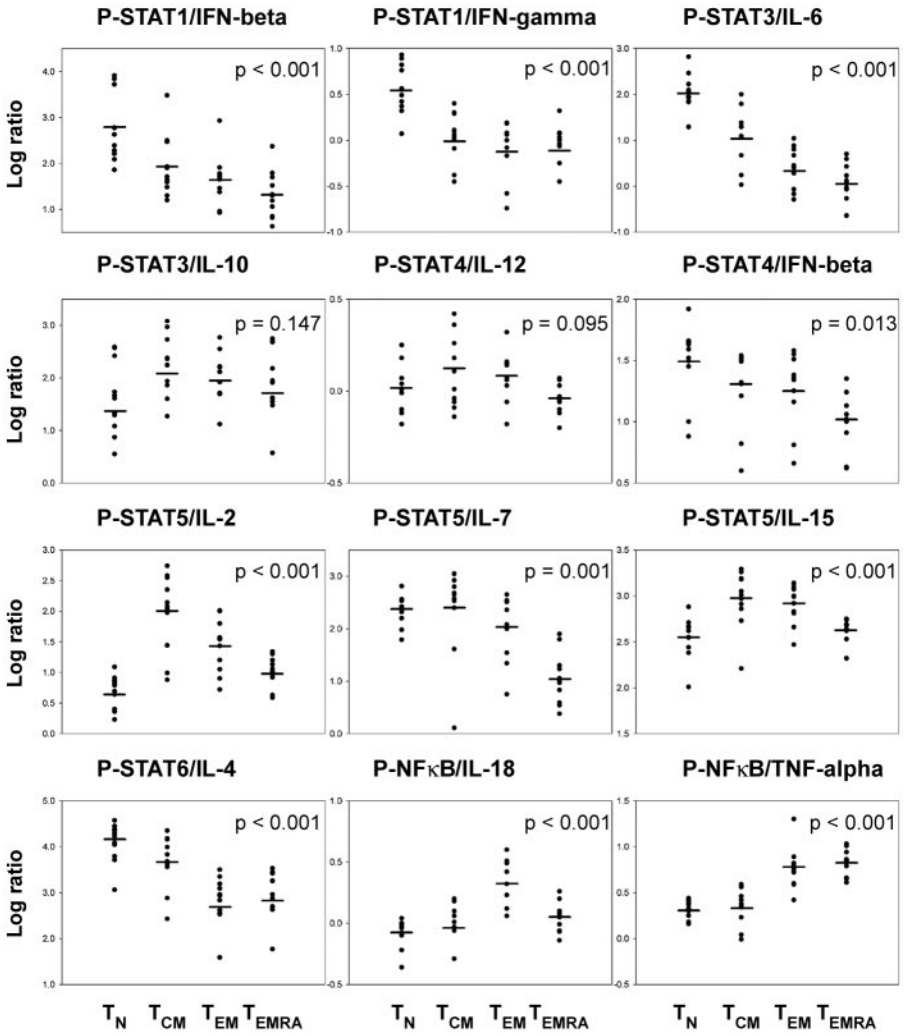

FIGURE 4. Differential activation of cytokine signaling pathways in CD8 T cell subsets. Target phosphorylations in CD8 T cell subsets to the indicated cytokines were analyzed by phospho-specific intracellular FACS. Log_2 ratios of fluorescent intensities (geometric mean) of stimulated cells relative to unstimulated cells are shown ($n = 10$). Mean phospho-responses for each cytokine-stimulated state are indicated by black bars. Values of p (determined by one-way ANOVA testing, $\alpha = 0.05$) are shown for each phospho-signaling node.

identified by selective expression of the IL-7Rα (40). Furthermore, a recent study found that STAT5 regulates the self-renewal and differentiation of human memory B cells (41). Therefore our results might explain why T_{CM} have a greater expansion potential and self-renewal capacity than effector memory cells, T_{EMRA} in particular. In contrast, we found that both effector memory subsets strongly express genes involved in CD8 T cell effector function. However, our data also show that the gene expression profile of T_{CM} is biased to some extent toward effector differentiation, characteristic of effector memory cells. Thus, mRNAs encoding effector molecules like perforin, granzyme A, IFN-γ, and RANTES were up-regulated in T_{CM} compared with T_N.

The lineage relationship between CD8 T cell subsets remains controversial. Our study is cross-sectional in design and therefore does not directly address questions relating to T cell lineage. It is however interesting to consider the results of our study in the light of recently proposed models. Lanzavecchia and colleagues (6) have suggested a signal strength model of T cell memory differentiation. According to this model, TCR signal strength determines the memory cell fate a naive T cells acquires: A low Ag dose leads to the differentiation $T_N \rightarrow$ noneffector $\rightarrow T_{CM}$, whereas a high Ag dose to $T_N \rightarrow$ effector $\rightarrow T_{EM}$ differentiation. Their work also suggests that human T_{CM} further differentiate into T_{EM} following Ag stimulation and into T_{EMRA} in response to homeostatic cytokines (9). The results of our microarray analysis showing that the gene expression profile of T_{CM} cells is largely intermediate between T_N and T_{EM} or T_{EMRA} subsets would be consistent with this type of model. In contrast, another model based on the idea that T_{CM} and T_{EM} are independent populations has been proposed by Pannetier and coworkers (19), who found that the TCR repertoires of influenza-specific T_{CM} and T_{EM} are largely distinct. We did not find many truly T_{CM}- and T_{EM}-specific genes and this argues against an independent T_{CM}/T_{EM} differentiation pathway. Finally, Ahmed and coworkers (18) have defined a linear differentiation pathway $T_N \rightarrow$ effector $\rightarrow T_{EM} \rightarrow T_{CM}$ in a murine model of acute LCMV infection. Interestingly, this $T_{EM} \rightarrow T_{CM}$ conversion does not occur in chronic LCMV infection (42). A second study by Pannetier and colleagues (43) using murine H-Y-specific CD8 T cells confirmed this linear differentiation pathway although there was also evidence for an independent T_{CM}/T_{EM} differentiation pathway. The observation that T_{CM} cells are intermediate between T_N and T_{EM} cells does not obviously support this type of linear differentiation model. However, the present study is cross-sectional in nature and therefore we do not exclude the possibility that T_{EM} convert to T_{CM}. Interesting questions about the plasticity of the genetic program of the CD8 memory T cell remain and further work will be needed to address these issues. Finally, it is noteworthy that the studies by Ahmed and Pannetier have not examined the T_{EMRA} subset in relation to T_{CM} and T_{EM} as we did in the present work. Effector memory cells re-expressing CD45RA form a sizeable population in human peripheral blood and are likely to have an important role in human CD8 T cell memory.

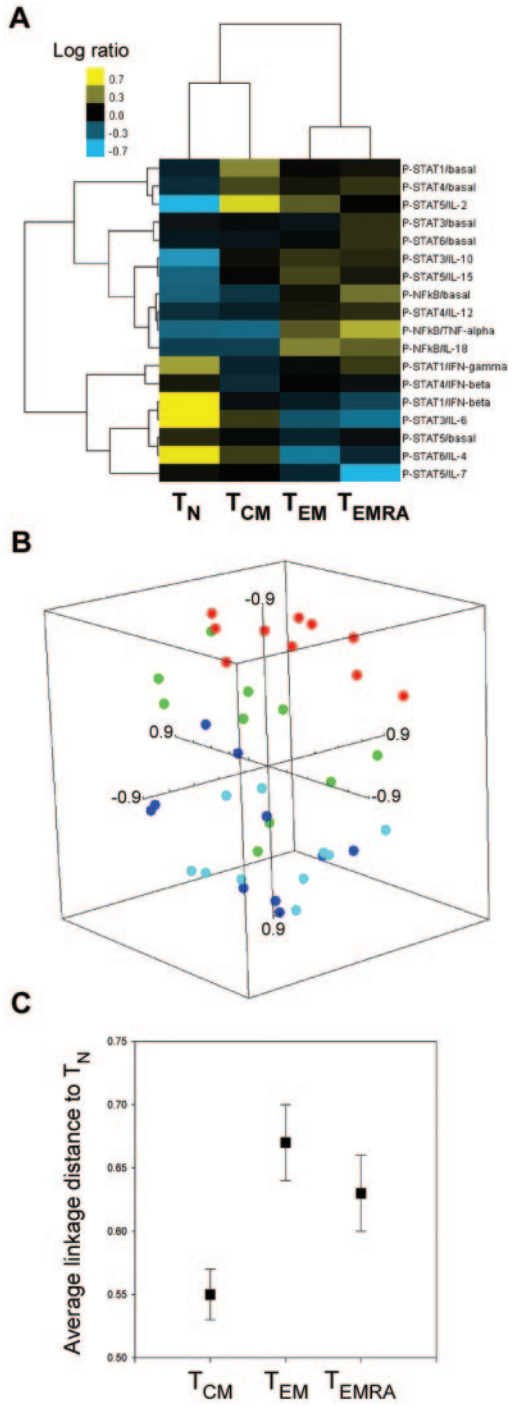

FIGURE 5. Cytokine signaling signatures of CD8 memory subsets. *A*, Hierarchical clustering of cytokine phospho-responses in CD8 T cell subsets. Complete linkage clustering using the Pearson correlation was conducted to define a 18-parameter biosignature for CD8 subsets. The color bar indicates the mean $\log_2$ ratios of cytokine-stimulated vs unstimulated phospho-specific fluorescent intensities from 10 donors. Basal responses are relative to the minimum among samples. *B*, MDS analysis of CD8 T cell subsets. The three-dimensional plot shows the between sample distances for 10 replicate CD8 T cell subset samples based on the 18-parameter biosignature from *A*. Pearson correlation was used as the distance metric. Each dot represents a single replicate sample. Color coding: T_N (red), T_{CM} (green), T_{EM} (dark blue), and T_{EMRA} (light blue). *C*, Average linkage distances between CD8 T_N and memory subsets. Average linkage distances between each CD8 memory T cell subset and T_N were calculated as described in *Materials and Methods* based on the 18-parameter biosignature from *A*. Error bars represent SEs (SD of pairwise linkages divided by the square root of the number of linkages).

In conclusion, our genomic and phospho-proteomic study demonstrates a dichotomy between CD8 T_{CM} and T_{EM}/T_{EMRA} cells at the molecular level and suggests that human T_{CM} cells represent an intermediate state between the T_N and the T_{EM}/T_{EMRA} populations in terms of CD8 memory differentiation and function. By defining molecular signatures for CD8 memory subsets, we provide a framework for the further molecular characterization of human CD8 T cell memory.

Acknowledgments

We thank Ann Atzberger for expert cell sorting, Hayley Woffendin of the LRF Microarray Facility for assistance in performing the GeneChip analysis, Sumit Bhattacharyya for submitting the microarray data to the EBI ArrayExpress database, and Charles Bangham for advice and reading of this manuscript.

Disclosures

The authors have no financial conflict of interest.

References

1. Sprent, J., and C. D. Surh. 2002. T cell memory. *Annu. Rev. Immunol.* 20: 551–579.
2. Kaech, S. M., E. J. Wherry, and R. Ahmed. 2002. Effector and memory T-cell differentiation: implications for vaccine development. *Nat. Rev. Immunol.* 2: 251–262.
3. Rocha, B., and C. Tanchot. 2004. CD8 T cell memory. *Semin. Immunol.* 16:305–314.
4. Hamann, D., P. A. Baars, M. H. G. Rep, B. Hooibrink, S. R. Kerkhof-Garde, M. R. Klein, and R. A. W. van Lier. 1997. Phenotypic and functional separation of memory and effector human $CD8^+$ T cells. *J. Exp. Med.* 186: 1407–1418.
5. Sallusto, F., D. Lenig, R. Foerster, M. Lipp, and A. Lanzavecchia. 1999. Two subsets of memory T lymphocytes with distinct homing potentials and effector functions. *Nature* 401: 708–712.
6. Sallusto, F., J. Geginat, and A. Lanzavecchia. 2004. Central memory and effector memory T cell subsets: function, generation, and maintenance. *Annu. Rev. Immunol.* 22: 745–763.
7. Hislop, A. D., N. H. Gudgeon, M. F. C. Callan, C. Fazou, H. Hasegawa, M. Salmon, and A. B. Rickinson. 2001. EBV-specific $CD8^+$ T cell memory: relationships between epitope specificity, cell phenotype, and immediate effector function. *J. Immunol.* 167: 2019–2029.
8. Tomiyama, H., T. Matsuda, and M. Takiguchi. 2002. Differentiation of human $CD8^+$ T cells from a memory to memory/effector phenotype. *J. Immunol.* 168: 5538–5550.
9. Geginat, J., A. Lanzavecchia, and F. Sallusto. 2003. Proliferation and differentiation potential of human $CD8^+$ memory T-cell subsets in response to antigen or homeostatic cytokines. *Blood* 101: 4260–4266.
10. Zippelius, A., G. Bioley, F.-A. Le Gal, N. Rufer, M. Brandes, P. Batard, M. de Smedt, J. Plum, D. E. Speiser, J.-C. Cerottini, et al. 2004. Human thymus exports naïve CD8 T cells that can home to nonlymphoid tissues. *J. Immunol.* 172: 2773–2777.
11. Huster, K. M., V. Busch, M. Schiemann, K. Linkemann, K. M. Kerksiek, H. Wagner, and D. H. Busch. 2004. Selective expression of IL-7 receptor on memory T cells identifies early CD40L-dependent generation of distinct $CD8^+$ memory T cell subsets. *Proc. Natl. Acad. Sci. USA* 101: 5610–5615.
12. Rufer, N., A. Zippelius, P. Batard, M. J. Pittet, I. Kurth, P. Corthesy, J.-C. Cerottini, S. Leyvraz, E. Roosnek, M. Nabholz, and P. Romero. 2003. Ex vivo characterization of human $CD8^+$ T subsets with distinct replicative history and partial effector functions. *Blood* 102: 1779–1787.
13. Champagne, P., G. S. Ogg, A. S. King, C. Knabenhans, K. Ellefsen, M. Nobile, V. Appay, G. P. Rizzardi, S. Fleury, M. Lipp, et al. 2001. Skewed maturation of memory HIV-specific CD8 T lymphocytes. *Nature* 410: 106–111.
14. Mueller, Y. M., S. C. De Rosa, J. A. Hutton, J. Witek, M. Roederer, J. D. Altman, and P. D. Katsikis. 2001. Increased CD95/Fas-induced apoptosis of HIV-specific $CD8^+$ T cells. *Immunity* 15: 871–882.
15. Lauvau, G., S. Vijh, P. Kong, T. Horng, K. Kerksiek, N. Serbina, R. A. Tuma, and E. G. Pamer. 2001. Priming of memory but not effector CD8 T cells by a killed bacterial vaccine. *Science* 294: 1735–1739.
16. Zaph, C., J. Uzonna, S. M. Beverly, and P. Scott. 2004. Central memory T cells mediate long-term immunity to *Leishmania major* in the absence of persistent parasites. *Nat. Med.* 10: 1104–1110.
17. Seaman, M. S., F. W. Peyerl, S. S. Jackson, M. A. Lifton, D. A. Grogone, J. E. Schmitz, and N. L. Letvin. 2004. Subsets of memory cytotoxic T lymphocytes elicited by vaccination influence the efficiency of secondary expansion in vivo. *J. Virol.* 78: 206–215.
18. Wherry, E. J., V. Teichgräber, T. C. Becker, D. Masopust, S. M. Kaech, R. Antia, U. H. von Adrian, and R. Ahmed. 2003. Lineage relationship and protective immunity of memory CD8 T cell subsets. *Nat. Immunol.* 4: 225–234.
19. Baron, V., C. Bouneaud, A. Cumano, A. Lim, T. P. Arstila, P. Kourilsky, L. Ferradini, and C. Pannetier. 2003. The repertoires of circulating human $CD8^+$ central and effector memory T cell subsets are largely distinct. *Immunity* 18: 193–204.

20. Petalidis, L., S. Bhattacharyya, G. A. Morris, V. P. Collins, T. C. Freeman, and P. A. Lyons. 2003. Global amplification of mRNA by template-switching PCR: linearity and application to microarray analysis. *Nucleic Acids Res.* 31: e142.
21. Simon, R., and A. Lam. 2004. BRB-ArrayTools User Guide, version 3.2. Biometric Research Branch, National Cancer Institute, http://linus.nci.nih.gov/brb.
22. Ye, Q-H., L-X. Qin, M. Forgues, P. He, J. W. Kim, A. C. Peng, R. Simon, Y. Li, A. I. Robles, Y. Chen, et al. 2003. Predicting hepatitis B virus-positive metastatic hepatocellular carcinomas using gene expression profiling and supervised machine learning. *Nat. Med.* 9: 416–423.
23. Irizarry, R. A., B. M. Bolstad, F. Collin, L. M. Cope, B. Hobbs, and T. P. Speed. 2003. Summaries of Affymetrix GeneChip probe level data. *Nucleic Acids Res.* 31: e15.
24. McShane, L. M., M. D. Radmacher, B. Freidlin, R. Yu, M. C. Li, and R. Simon. 2002. Methods of assessing reproducibility of clustering patterns observed in analyses of microarray data. *Bioinformatics* 18: 1462–1469.
25. Wang, H-W., M. W. B. Trotter, D. Lagos, D. Bourboulia, S. Henderson, T. Maekinen, S. Elliman, A. M. Flanagan, K. Alitalo, and C. Boshoff. 2004. Kaposi sarcoma herpesvirus-induced cellular reprogramming contributes to the lymphatic endothelial gene expression in Kaposi sarcoma. *Nat. Genet.* 36: 687–693.
26. Wright, G. W., and R. Simon. 2003. A random variance model for detection of differential gene expression in small microarray experiments. *Bioinformatics* 19: 2448–2455.
27. Tusher, V. G., R. Tibshirani, and G. Chu. 2001. Significance of microarray analysis applied to the ionizing radiation response. *Proc. Natl. Acad. Sci. USA* 98: 5116–5121.
28. Khatri, P., S. Draghici, G. C. Ostermeier, and S. A. Krawetz. 2002. Profiling gene expression using Onto-Express. *Genomics* 79: 266–270.
29. Perez, O. D., P. O. Krutzik, and G. P. Nolan. 2004. Flow cytometric analysis of kinase signaling cascades. *Methods Mol. Biol.* 263: 67–94.
30. Trambas, C. M., and G. M. Griffiths. 2003. Delivering the kiss of death. *Nat. Immunol.* 4: 399–403.
31. Glimcher, L. H., M. J. Townsend, B. M. Sullivan, and G. M. Lord. 2004. Recent developments in the regulation of cytolytic effector cells. *Nat. Rev. Immunol.* 4: 900–911.
32. Perez, O. D., and G. P. Nolan. 2002. Simultaneous measurement of multiple active kinase states using polychromatic flow cytometry. *Nat. Biotechnol.* 20: 155–162.
33. Irish, J. M., R. Hovland, P. O. Krutzik, O. D. Perez, O. Bruserud, B. T. Gjertsen, and G. P. Nolan. 2004. Single cell profiling of potentiated phospho-protein networks in cancer cells. *Cell* 118: 217–228.
34. Holmes, S., M. He, T. Xu, and P. P. Lee. 2005. Memory T cells have gene expression patterns intermediate between naïve and effector. *Proc. Natl. Acad. Sci. USA* 102: 5519–5523.
35. Kaech, S. M., S. Hemby, E. Kersh, and R. Ahmed. 2002. Molecular and functional profiling of memory CD8 T cell differentiation. *Cell* 111: 837–851.
36. Appay, V., P. R. Dunbar, M. Callan, P. Klenerman, G. M. A. Gillespie, L. Papagno, G. S. Ogg, A. King, F. Lechner, C. A. Spina, et al. 2002. Memory $CD8^+$ T cells vary in differentiation phenotype in different persistent virus infections. *Nat. Med.* 8: 379–385.
37. van Lier, R. A. W., I. J. M. ten Berge, and L. E. Gamadia. 2003. Human $CD8^+$ T-cell differentiation in response to viruses. *Nat. Rev. Immunol.* 3: 1–8.
38. Jameson, S. C. 2002. Maintaining the norm: T-cell homeostasis. *Nat. Rev. Immunol.* 2: 547–556.
39. Schluns, K. S., and L. Lefrancois. 2003. Cytokine control of memory T-cell development and survival. *Nat. Rev. Immunol.* 3: 269–279.
40. Kaech, S. M., J. T. Tan, E. J. Wherry, B. T. Konieczny, C. D. Surh, and R. Ahmed. 2003. Selective expression of the interleukin 7 receptor identifies effector CD8 T cells that give rise to long-lived memory cells. *Nat. Immunol.* 4: 1191–1198.
41. Scheeren, F. A., M. Naspetti, S. Diel, R. Schotte, M. Nagasawa, E. Wijnands, R. Gimeno, F. A. Vyth-Dreese, B. Blom, and H. Spits. 2005. STAT5 regulates the self-renewal capacity and differentiation of human memory B cells and controls Bcl-6 expression. *Nat. Immunol.* 6: 303–313.
42. Wherry, E. J., D. L. Barber, S. M. Kaech, J. N. Blattman, and R. Ahmed. 2004. Antigen-independent memory CD8 T cells do not develop during chronic viral infection. *Proc. Natl. Acad. Sci. USA* 101: 16004–16009.
43. Bouneaud, C., Z. Garcia, P. Kourilsky, and C. Pannetier. 2005. Lineage relationships, homeostasis, and recall capacities of central- and effector-memory CD8 T cells in vivo. *J. Exp. Med.* 201: 579–590.